

Effect of carbon nanotubes support on band gap energy of MgO nanoparticles

L. Sohrabi · F. Taleshi · R. Sohrabi

Received: 19 April 2014 / Accepted: 24 June 2014 / Published online: 1 July 2014
© Springer Science+Business Media New York 2014

Abstract In this study, the effect of carbon nanotube supports (CNT) on the morphology and band gap of MgO nanoparticles was studied. The synthesis of MgO nanoparticles on the surface of CNT supports was carried out by direct precipitation method and using magnesium nitrate in aqueous solutions containing CNT. The prepared samples were characterized using X-ray diffraction. The optical properties of the nanoparticles were studied using UV–Vis spectrometer. The results indicated that the presence of CNTs decrease the average size of the MgO nanoparticles. Also the use of CNTs as support has reduced the band gap energy of MgO nanoparticles, considerably.

1 Introduction

In recent years, new types of nanomaterial have attracted the attention of many researchers [1, 2]. The size reduction of particles in nanoscale increases the ratio of surface to volume and causes the emergence of quantum effects in nanoparticles. This change in scale can have a significant impact on the physical behavior of material [3]. Magnesium oxide nanoparticles have unique properties such as; optical, electronic, thermal, and chemical ones [3–5]. These nanoparticles can be used as catalysts to accelerate chemical reactions, for the purposes such as detoxification, the production of antibacterial and thermal materials [6–8].

Recently, researchers used several methods for the synthesis of MgO nanoparticles with different geometric shapes, as nano-fibers, nano-plates, nanowires and volumetric porous nanostructures [4, 5, 9, 10]. On the other hand, CNTs due to their total unique properties e.g. electronic, thermal, adsorption, mechanical and chemical stability, will definitely lead us to the use of these properties [11–13]. Due to their high surface to volume ratio, they can be used as an appropriate support to control nanoparticle size and considered as an important influencing factor on their physical properties [14–17]. The combination of CNTs with MgO in nanoscale creates new MgO–CNTs nanocomposite materials. The prepared nanocomposite has the chemical and physical properties of common practice between CNTs and MgO. Joint properties can improve the performance of prepared nanocomposite. So far, several attempts have been made to use CNTs as a support for the growth of MgO nanoparticles and prepare MgO–CNTs nanocomposite powder [16–18]. Among various methods, the direct precipitation method is simple, low cost and due to having control on synthesis process is the most appropriate one [19]. However there always exist two fundamental problems in utilizing CNTs as support for nucleation and growth of nanoparticles [15, 19, 20]. One is the non-uniform distribution of nanoparticles on the surface of carbon nanotubes (CNTs) and the other is the lack of proper wetting of CNTs surface (to create a strong chemical bond and adherence of nanoparticles to the wall surface of CNTs) [19, 21]. Failure to achieve such conditions can affect the physical and chemical properties of nanoparticles. Thus, activation of the nanotube surface for proper interaction between their surfaces with material is necessary. Activation of CNTs surface is generally conducted using a chemical oxidation processes and causes various functional groups such as, –OH, –C=O, C–O and

L. Sohrabi · F. Taleshi (✉)
Department of Applied Science, Qaemshahr Branch, Islamic Azad University, Qaemshahr, Iran
e-mail: far.taleshi@gmail.com

R. Sohrabi
Department of Chemistry, Qaemshahr Branch, Islamic Azad University, Qaemshahr, Iran

–COOH, that are considered as sites for nucleation of metal ions [19, 21, 22].

In this study, CNTs was used as a support for nucleation and growth of MgO nanoparticles through direct deposition method. The functionalized of CNTs characterized using infrared spectroscopy instrument (FT-IR, Shimadzu-8400s). The effect of CNTs' support on the size of MgO nanoparticles were studied by X-ray diffraction apparatus (XRD, GBC, $\text{Cu}_{K-\alpha}$, $\lambda = 1.54 \text{ \AA}$). Also, the optical properties and band gap energy of MgO nanoparticles were studied by using (UV–Vis, Spekol 2000) spectroscopy.

2 Experimental procedure

To perform the experiment, different concentration MgO/CNTs nanocomposite powders with ratio of 1:0, 2:1, 1:1, 1:2, 1:4 and 1:8 were prepared by using CNT support in solution during the synthesis of powders. In order to synthesize the samples, 50 cc distilled water containing reducing sodium hydroxide ($\text{pH} = 10.5$) and a desired amount of functionalized CNTs were added into it, then was placed under ultrasonic waves for 10 min. To prepare a solution containing metal ions Mg^{2+} , 1.8 g of magnesium nitrate salt was dissolved in 100 cc distilled water. During rotation process aqueous solutions containing reducing sodium hydroxide (first and second samples) at $50 \text{ }^\circ\text{C}$, solution containing $\text{Mg}(\text{NO}_3)_2 \cdot 6\text{H}_2\text{O}$ salt was added in gummy form to it. During synthesis process the rate of adding salt solution was kept constant in 20 ml/h. Also during the synthesis process by adding sodium hydroxide solution, pH of the solution was kept constant to the 10.5 (to compensate its amount reduction due to the decomposition of magnesium oxide). When the salt solution was finished and saturation process was completed, the obtained sediment was rotated at room temperature for 15 h. At the end of the mentioned step, the prepared sediment was leached with distilled water several times to neutral the material from basic mood ($\text{pH} = 7.5$). The obtained wet product was dried for 2 h at $120 \text{ }^\circ\text{C}$ then was calcined at room temperature $450 \text{ }^\circ\text{C}$ for 2.5 h. Furnace temperature was increased from room temperature to $450 \text{ }^\circ\text{C}$ uniformly and with a linear gradient as $10 \text{ }^\circ\text{C}/\text{min}$.

3 Results and discussion

To study the formation of functional groups on the surface of CNTs, FT-IR spectrum was prepared. Figure 1 shows the FT-IR spectra of the CNTs before and after the acid pickling process. The peaks in the FT-IR spectra shows bond formation of functional groups O–C=O, C–O–O, C–O, and C=O respectively, at wavelength of 1,210, 1,415,

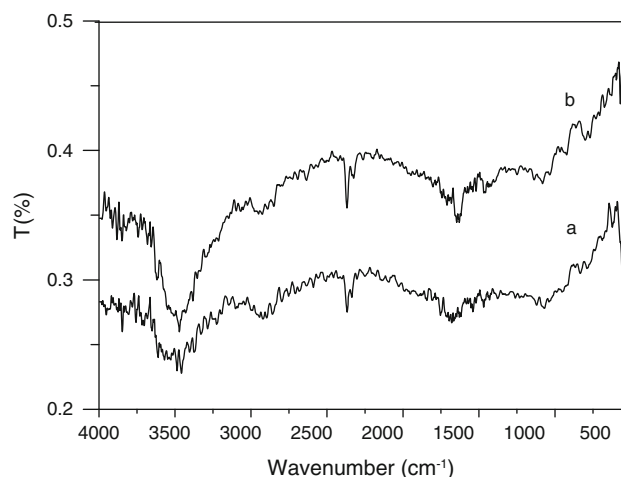


Fig. 1 FT-IR spectra of CNTs; (a) before purification and (b) after the purification process

1,475 and $1,720 \text{ (cm}^{-1}\text{)}$ during the thermal and ultrasonic oxidation processes in HNO_3 and H_2SO_4 acid solutions [19, 21, 22]. These functional groups play an important role in the nucleation and formation of MgO nanoparticles. Due to formation of –OH functional group in $\text{Mg}(\text{OH})$ and O–C=O, C–O–O, C–O and C=O functional groups on the surface of CNTs, MgO/CNTs composite by chemical and physical bonds such as van der Waals, H bonding and other bonds are formed, e.g. –OH bond in $\text{Mg}(\text{OH})$ may be reacted with –OH agent of –COOH group located on the surface of CNTs causes the forming of H_2O in composites. Therefore strong covalent bonds C–O–MgO and O=C–O–MgO can be formed between the surface of the nanotubes with magnesium ions. Due to the high surface area CNTs, the formation of such bonds can be considered as a basis for the formation of nanocomposite powder of MgO/CNTs.

To study the crystalline structure of MgO nanoparticles and MgO/CNTs nanocomposite XRD spectra and MgO/CNTs nanocomposite were obtained from synthesized samples. Figure 2 shows XRD spectra of MgO/CNTs nanocomposite powders in the angular range of $2\theta = 5^\circ - 60^\circ$. As Fig. 2a, for pure MgO sample with ratio of 1/0, peaks located at 37.04 and 42.92 , respectively depending on the plans of (111) and (200) of MgO nanoparticles with fcc crystal structure [17–19]. The mean value of nanocrystalline dimensions was determined using the Debye–Scherrer equation [23]:

$$D = \frac{0.9\lambda}{\beta \cos \theta} \quad (1)$$

Where D is average size of nanocrystalline, λ is the wavelength of X-rays, β is full-width of half maximum peak (FWHM) in radians and θ the place of maximum peak. The mean value of nanocrystalline MgO dimensions was obtained 28.6 nm.

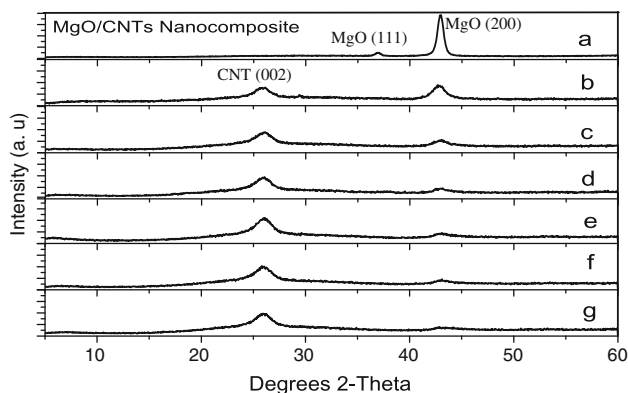


Fig. 2 XRD patterns of MgO/CNTs nanocomposites with different weight ratios of MgO to CNTs; (a) 1/0, (b) 2/1, (c) 1/1, (d) 1/2, (e) 1/4 and (f) 1/8, calcined at 400 °C

As Fig. 2b–g, they shows the XRD spectra of MgO/CNTs nanocomposite with 1/1, 2:1, 1/2, 1/4 and 1/8 ratios of MgO to CNTs, respectively. According to the XRD pattern, the peak at $2\theta = 26.7^\circ$ is related to graphite structure of CNTs for (002) plans [19] and other maximum peak located at 42.92° was dependent on MgO nanoparticles [18, 19]. It also can be seen that using CNTs as a support, the maximum peak height depended on the MgO nanoparticles has been reduced and its width increased. The mean value of nanocrystalline MgO dimensions formed on CNTs' surface for weight ratio of 2:1, 1:1, 1:2, 1:4 and 1:8 were determined 14.3, 13.2, 12.4, 11.3 and 10.1 nm, respectively. By comparing the size of nanocrystalline MgO in two different syntheses (in the absence and presence of CNTs support) it can be seen that the presence of CNTs support substantially reduces the size of MgO nanocrystalline. The reduction of MgO nanoparticles dimensions along with the presence of CNTs support with unique properties can have a significant impact on the physical properties of nanoparticles.

Morphology of prepared MgO powder and MgO/CNTs nanocomposite with weight ratio of 1/2 and calcined at 400 °C was analysed by SEM images and is shown in Fig. 3. As Fig. 3a, because of surface activity, MgO nanoparticles are seen as dense aggregates and make large particles. It is obvious that the aggregated particles have irregular shape. As SEM images (Fig. 3b), by using CNTs as a support, they were prevent to aggregation of MgO nanoparticles and they was made nanorode of MgO nanoparticles. This unique morphology can effect on physical and chemical properties of MgO/CNTs nanocomposite. Also, the well-distributed nanoparticles deposited on surface of the CNTs demonstrate that the CNTs pretreatment processing was effective, which resulted in many active sites on the CNTs. Accordingly, UV–Vis spectroscopy was prepared to study the effect of CNTs

support on optical absorption and the band gap energy of MgO nanoparticles and MgO/CNTs nanocomposites samples. Figure 4 show the UV–Vis spectra of MgO nanoparticles and MgO/CNTs nanocomposite. According to UV–Vis spectra, intensity of UV–Vis absorption is dependence to concentration of CNTs directly.

The optical band gap (E_g) can be calculated by the Tauc equation [24], on the basis of the optical absorption spectra:

$$(\alpha hv)^{1/n} = B(hv - E_g) \quad (2)$$

where α is the absorption coefficient, hv is the incident photons energy and n is an integer power, which characterizes the electronic transition during absorption processes in the K-space. Particularly, n is 1/2, 3/2, 2 and 3 for direct allowed, direct forbidden, indirect allowed and indirect forbidden transitions, respectively. The value of B depends on the transition probability that can be considered constant within the optical frequency range. The usual method for the determination of E_g involves plotting $(\alpha hv)^{1/n}$ against (hv) .

The Tauc plot with $n = 1/2$ for the direct allowed band gap corresponding to the MgO UV–Vis spectrum (Fig. 4) is shown in Fig. 5. Hence, the optical band gap for the absorption peak can be obtained by extrapolating the linear portion of the $(\alpha hv)^2_{-hv}$ curve. The direct band gap energy of MgO is 5.5 eV. Band gap energy of both samples is smaller than the band gap energy of bulk MgO (7.8 eV) [25]. As Fig. 5b, it can be seen that the band gap energy of MgO/CNTs nanocomposites decrease by increasing of CNTs concentration in nanocomposites and they are smaller than the band gap energy of the MgO nanoparticles. Thus, nano crystallites of MgO in both samples exhibit band gap energies smaller than the bulk. The experimental results show that the different crystallite size and CNTs can influence the band gap energies of the MgO materials. By application of CNTs as a support of MgO nanoparticles, this effect is probably due to increase in chemical defects or vacancies present in the intergranular regions and also chemical interaction between CNTs and MgO nanoparticles, generating a new energy level to reduce the band gap energy [26]. The MgO/CNTs nanocomposites with lower band gap energy are optically active and have been extensively used in the field of photo-oxidation catalysis for environmental cleanup and solar sell.

In comparison with bulk MgO ($E_g = 7.8$ eV), the decrease in the values of band gap indicated that MgO with the nanoscale size showed a red shift in their spectra due to the quantum confinement effects. The shift of band-gap energy ΔE and nanoparticles size were used for the estimation of the reduced effective mass as in terms of the well-known Brus equation [27, 28]:

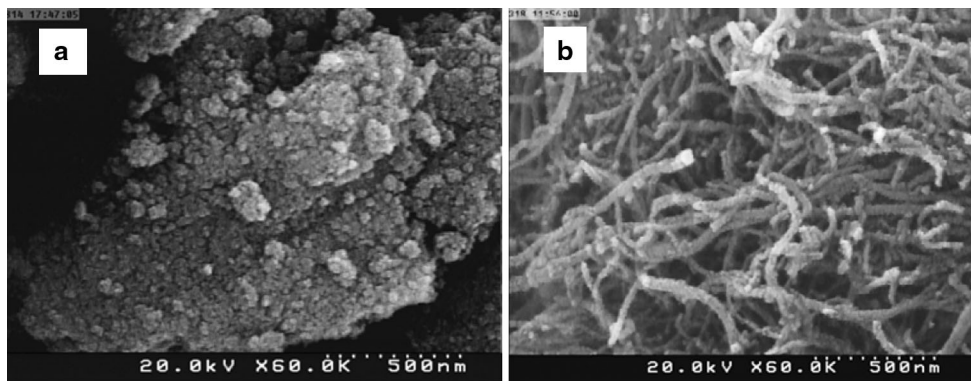


Fig. 3 SEM images of pure MgO powder **a** and MgO/CNTs nanocomposite (with weight ratio of 1/2)

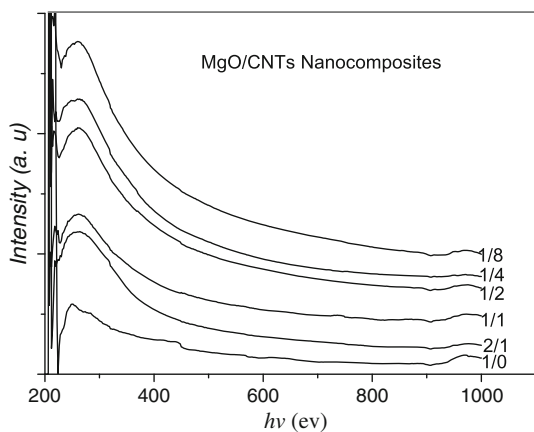


Fig. 4 UV-Vis spectra of MgO/CNTs nanocomposite powders with different weight ratio of MgO to CNTs, in the calcined temperature 400 °C

$$\Delta E = E_g(nano) - E_g(bulk) = \frac{h^2}{8R^2} \left(\frac{1}{m_e^*} + \frac{1}{m_h^*} \right) - \left(\frac{1.8e^2}{4\pi\epsilon\epsilon_0 R} \right) \quad (3)$$

where E_g (nano) and E_g (bulk) are the band gap energies of nanosized and bulk semiconductors, respectively, h is the Planck's constant, ϵ is the dielectric constant of the material, R is the mean radius of the nanoparticles, m_e^* and m_h^* are the effective mass of electrons and holes. The first term represents the energy of localization. The second term represents the Coulombic attraction effect and can be neglected because of its very small contribution in the Brus equation. In our case, the red shift in the band gap is about 4.35 for pure MgO and 4.45 for MgO/CNTs nanocomposite (with 1:1 ratio), also from XRD analysis the radius particles size is about 14.3 and 6.6 nm, respectively).

Using above equation, we found the reduced effective mass $\frac{1}{\mu} = \left[\frac{1}{m_e^*} + \frac{1}{m_h^*} \right]$ equal to 0.0038 m_0 and 0.0081 m_0 for our prepared MgO/CNTs nanocomposite with ratios of 1/0 and 1/1, respectively, where m_0 is the free electron mass.

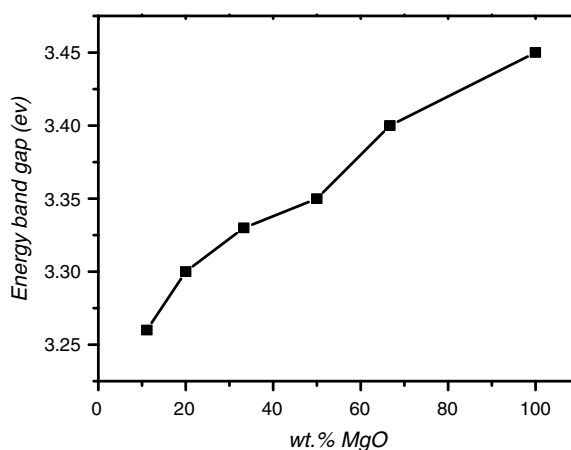
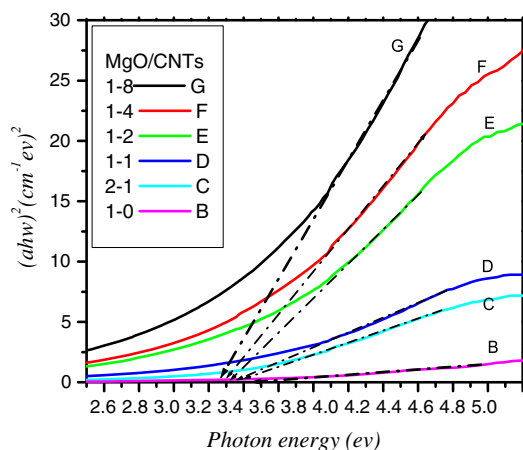


Fig. 5 Extrapolating the linear portion of the $(\alpha hv)^2_{-}hv$ curve for pure MgO nanoparticles and MgO/CNTs nanocomposite powder with different weight ratios of MgO to CNTs

4 Conclusion

In this study, the synthesis of MgO nanoparticles and MgO₂/CNTs nanocomposite powder was carried out by magnesium nitrate precursor using the direct precipitation method. The results show that application of CNTs as a support was decreased the size of MgO nanoparticles. Also, the results of optical spectra show that the presence of CNTs alters the absorption area towards higher wavelengths and the band gap of bulk MgO (7.8 eV) has been decrease to its' minimum value 3.27 eV.

Acknowledgments The authors would like to acknowledge Islamic Azad University of Qaemshahr and the Iranian National Nanotechnology Initiation Council (INNIC) for their financial support of this project.

References

1. E.T. Thostenson, Z. Ren, T.W. Chou, *Compos. Sci. Technol.* **61**, 1899 (2001)
2. B. Hea, M. Wang, W. Sun, Z. Shen, *Mater. Chem. Phys.* **95**, 289 (2006)
3. R. Kakkar, P.N. Kapoor, K.J. Klabunde, *J. Phys. Chem. B* **108**, 18140 (2004)
4. L.D. Zhang, J.M. Mou, *Nano-Materials and Nano-Structure 1* (2001)
5. D. Kumar, V.B. Reddy, B.G. Mishra, R.K. Rana, M.N. Nadagouda, R.S. Varma, *Tetrahedron* **63**, 3093 (2007)
6. R. Kakkar, P.N. Kapoor, K.J. Klabunde, *J. Phys. Chem. B* **110**, 25941 (2006)
7. L. Huang, D.Q. Li, Y.J. Lin, M. Wei, D.G. Evans, X. Duan, *J. Inorg. Biochem.* **99**, 986 (2005)
8. G.A. Slack, *Phys. Rev.* **126**, 427 (1962)
9. W. Wang, X. Qiao, J. Chen, H. Li, *Mater. Lett.* **61**, 3218–3220 (2007)
10. J.A. Wang, O. Novaro, X. Bokhimi, T. Lopez, R. Gomez, J. Navarrete, M.E. Llanos, E. Lopez-Salinas, *Mater. Lett.* **35**, 317 (1998)
11. M. Paradise, T. Gogswami, *Mater. Des.* **28**, 1477 (2007)
12. T. Wei, Z. Fan, G. Luo, F. Wei, *Mater. Lett.* **62**, 641 (2008)
13. R.P. Raffaele, B.J. Landi, J.D. Harris, S.G. Bailey, A.F. Hepp, *Mater. Sci. Eng. B* **116**, 233 (2005)
14. L. Chen, B.L. Zhang, M.Z. Qu, Z.L. Yu, *Powder Technol.* **154**, 70 (2005)
15. K. Hernadi, E. Ljubovic, J.W. Seo, L. Forro, *Acta Mater.* **51**, 1447 (2003)
16. S.B. Ma, K.Y. Ahn, E.S. Lee, K.H. Oh, K.B. Kim, *Carbon* **45**, 375 (2007)
17. H. Yue, X. Huang, Y. Yang, *Mater. Lett.* **62**, 3388 (2008)
18. K. Soumitra, C. Subhadra, *J. Nanosci. Nanotechnol.* **6**, 1447 (2006)
19. F. Taleshi, A.A. Hosseini, *J. Nanostruct. Chem.* **3**, 4 (2012). doi:[10.1186/2193-8865-3-4356](https://doi.org/10.1186/2193-8865-3-4356)
20. A.M.K. Esawi, M.A.E. Borady, *Compos. Sci. Technol.* **68**, 486 (2008)
21. L. Chen, B. Zhang, M. Qu, Z. Yu, *Powder Tech.* **154**, 70 (2005)
22. L. Zhao, G.L. Novel, *Carbon* **42**, 423 (2004)
23. K. Venkateswarlu, A. Chandra Bose, N. Rameshbabu, *Phys. B* **405**, 4256 (2010)
24. J. Tauc, *Amorphous and Liquid Semiconductors* (Plenum Press, New York, 1974)
25. A. Moses Ezhil Raj, L.C. Nehru, M. Jayachandran, C. Sanjeeviraja, *Cryst. Res. Technol.* **42**, 867 (2007)
26. F. Taleshi, A. Pahlavan, *J. Mater. Sci. Mater. Electron.* doi:[10.1007/s10854-014-1894-2](https://doi.org/10.1007/s10854-014-1894-2)
27. L.E. Brus, *J. Phys. Chem.* **79**, 5566 (1983)
28. L.E. Brus, *J. Phys. Chem.* **80**, 4403 (1984)